Coating of the HEFT telescope mirrors: method and results

Carsten P. Jensen, Kristin K. Madsen, Hubert C.M. Chen, Finn Erland Christensen, Eric Ziegler

Carsten P. Jensen, Kristin K. Madsen, Hubert C.M. Chen, Finn Erland Christensen, Eric Ziegler, "Coating of the HEFT telescope mirrors: method and results," Proc. SPIE 4851, X-Ray and Gamma-Ray Telescopes and Instruments for Astronomy, (11 March 2003); doi: 10.1117/12.461315

SPIE.

Event: Astronomical Telescopes and Instrumentation, 2002, Waikoloa, Hawai'i, United States

Coating of the HEFT telescope mirrors. Method and results.

Carsten P. Jensen[a], Kristin K. Madsen[a], Hubert C. Chen[b] Finn E. Christensen[a], Eric Ziegler[c]

[a]Danish Space Research Institute, Copenhagen, Denmark,

[b]California Institute of Technology, Pasadena, California,

[c]European Synchrotron Radiation Facility, Grenoble, France.

ABSTRACT

We report on the coating of depth graded W/Si multilayers on the thermally slumped glass substrates for the HEFT flight telescopes. The coatings consists of several hundred bilayers in an optimized graded power law design with stringent requirements on uniformity and interfacial roughness. We present the details of the planar magnetron sputtering facility including the optimization of power, Ar pressure and collimating geometry which allows us to coat the several thousand mirror segments required for each telescope module on a time schedule consistent with the current HEFT balloon project as well as future hard X-ray satellite projects. Results are presented on the uniformity, interfacial roughness, and reflectivity and scatter at hard X-ray energies.

Keywords: X-ray multilayers, hard X-ray telescopes, planar magnetron sputtering

1. INTRODUCTION

The High Energy Focusing Telescope (HEFT) is a balloon borne mission, which employs focusing optics in the hard X-ray band (20 - 70 keV) for sensitive observations of astrophysical sources. The primary scientific objectives include imaging and spectroscopy of ^{44}Ti emission in young supernova remnants, and sensitive hard X-ray observations of obscured Active Galactic Nuclei[1]. The focusing optic is based on depth graded W/Si multilayer coatings[2, 3] deposited on thermally slumped thin glass mirror segments[4, 5]. The HEFT telescope is a conical approximation to a Wolter-I geometry containing 72 mirror shells per telescope module varying in radius from 40 mm to 120 mm. Each mirror shell is divided into 5 mirror segments. Each shell, front and back, is 200 mm in the direction of the optical axis but is each divided into two 100 mm long segments to ensure better imaging performance of the telescope[6]. Thus each telescope module is made up of 1440 mirror segments. The complete design and mounting scheme is described in Koglin et al[6]. A prototype with realistic dimensions containing a few mirror shells have demonstrated subarcminute-imaging[6]. Once fully instrumented the HEFT balloon payload will carry several telescope modules. This requires that thousands of mirror segments must be coated in a relatively short period of time. To meet this requirement we have at the Danish Space Research Institute (DSRI) established a research and production coating facility. The facility is based on a planar magnetron sputtering arrangement. The next section describes the facility, the coating design, and the following section gives examples of typical soft and hard X-ray reflectance data as well as hard X-ray scatter data from coated flight mirrors.

2. COATING FACILITY

The coating facility at DSRI is optimized to make multilayer coatings that meet the strict quality requirements for HEFT or other hard X-ray missions and on the same time have a high throughput that make the production of the large

X-Ray and Gamma-Ray Telescopes and Instruments for Astronomy, Joachim E. Trümper, Harvey D. Tananbaum, Editors, Proceedings of SPIE Vol. 4851 (2003)

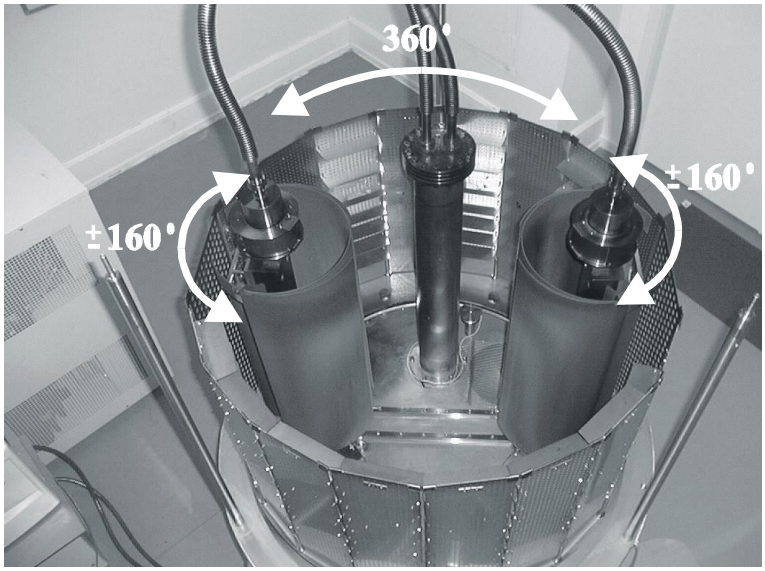

Fig. 1: Looking down in to the multilayer coating facility. The two 500 mm tall planar DC magnetron sources can be rotated ±160° from "open" position (as shown in the photography) so they coat into a screen. The sample ring, with a diameter of 1 m, holds 16 sample mounting plates and two dummy plates (in front of the cathodes on the photography) and can be rotated 360°. Each sample mounting plates are 600 mm tall and 150 mm wide.

number of mirror segments possible in the required time frame. The facility is a bell-jar vacuum chamber with a diameter of 1 m and it is 1.2 m tall. It consists of 2 planar DC magnetron sources that are pointing outwards and a sample ring where the substrates are mounted facing inwards, all three can rotate, see Fig. 1. The targets are 500 mm tall and 38 mm wide. The cathodes can be rotated 160° away from "open" position (see Fig. 1) so they sputter into the screen and no materials are then deposit on the substrates. When the coating parameters, Ar pressure and applied power to the two cathodes, have been decided the thickness of each of the two materials are controlled by the rotation speed of the sample ring. On the sample ring there are 16 mounting plates, each 600 mm tall and 150 mm wide, and two dummy plates also 600 mm tall but 240 mm wide. During a HEFT coating the rotation time for a full rotation is between one and a half minute and 20 minutes as the period of the coating varies from the smallest *d*-spacings (~2.3 nm) to the largest (30 nm).

The coatings are computer controlled and there is several different coating modes[7]. Here will only the mode used for the calibration coating and the flight coating be described briefly. The calibration mode is designed to make 8 different 10 bilayer constant *d*-spacing coatings in one run, where *d* is the total thickness of one layer of the low Z material and one layer of the high Z material, the bilayer thickness. Calibration samples, which are a combination of Si wafers with a roughness of 0.30 nm and flight substrates, are placed on every second of the sample mounting plates. A dummy plate is placed in front of one of the magnetrons, the magnetron is opened, and at 8 different speeds the 8 calibration sample plates are rotated past the cathode. The empty sample mounting plates are used for acceleration and deacceleration. After one full rotation the magnetron is closed and the dummy plate is rotated to the other magnetron. The magnetron with the lowest coating rate is running at maximum power and the power applied to the other magnetron is adjusted so the desirable ratio between the two materials, Γ, is obtained. From X-ray measurements the thickness of the bilayer can be calculated, Γ controlled, and a calibration file can quickly be generated.

To decrease the coating time for the flight coatings both W and Si are coated on the same time. This is the reason Γ is controlled by the applied power and not with different rotation speed when the calibration coating is made. When doing the flight coatings the two dummy plates are placed in front of the two magnetrons. Both magnetrons are then opened and when the sample ring has made one full rotation a complete bilayer has been coated. Half off the samples have W as top coating and the other half Si. When all the bilayers have been coated the W cathode is closed and the Si cathode coat a top layer on half of the samples. Because the flight coatings are depth graded coatings with a large numbers of

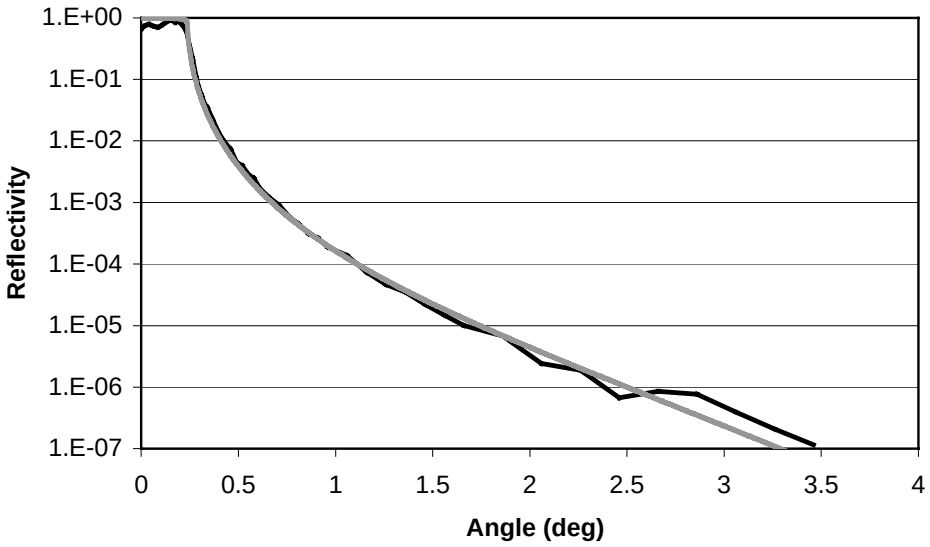

Fig. 2: The reflectivity as function of grazing incidence angle measured with 8 keV on a flight mirror before coating. The black line is the experimental data and the gray line is the fit giving a roughness of 0.36 nm.

layers the only difference between the samples are a small shift in bilayer thickness. This shift is so small that we have not been able to see the effect on the graded flight coatings.

We are running the magnetron with Si at 900 W and the magnetron with W at 260 W at an Ar pressure of 0.49 Pa (3.7 mTorr) giving $\Gamma = 0.4$ as used in the flight coatings, see below. The background pressure in the chamber is better than $7*10^{-5}$ Pa ($5*10^{-7}$ Torr) and the target sample distance is 108 mm.

3. COATING DESIGN

The coatings for HEFT are depth graded W/Si multilayers where the bilayers thickness distribution is defined using a power law distribution[8]

$$d_i = \frac{a}{(b+i)^c},$$

where *a*, *b*, and *c* are constants and *i* is the bilayer index ranging from 1 to *N*, the total number of bilayers, where $i = N$ is the bilayer next to the substrate. It is more convenient to define the minimum *d*-spacing, d_{min}, (closest to the substrate) and the maximum *d*-spacing, d_{max}, for which the parameters *a* and *b* are uniquely determined. The thickness of the high Z material (W in this case) is set to a constant fraction, Γ, of the total bilayer thickness.

The 72 shells of each telescope are divided into 10 groups for multilayer optimization purposes. The 10 groups have been separately optimized; the optimization and the designs of each of the 10 groups have been described elsewhere[9]. The number of bilayers goes from 125 for the innermost mirror group and up to 312 for the outermost groups. The minimum *d*-spacing is 3.33 nm and the maximum *d*-spacing is 29.76 nm for the innermost mirror group and 2.30 nm and 11.07 nm for the outermost mirror group. The power of the power law design, c, and Γ are also optimized for each mirror group and typical values are $c = 0.23$ and $\Gamma = 0.39$[9]. The optimization results in a total thickness for all the coatings between 0.5 μm and 1.0 μm[9].

a 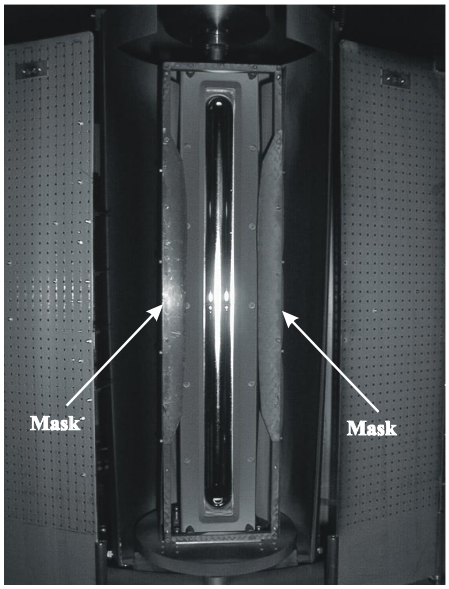

b 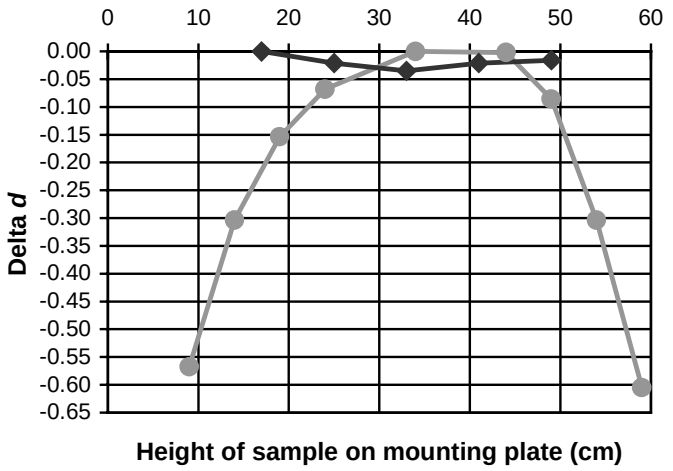

Fig. 3a: The DC magnetron seen in "open" position, the dummy plate has been removed. The target is 500 mm tall and 38 mm wide. The two masks, mounted 48 mm from the target, results in a homogeneous coating area that is 350 mm tall. b: Delta *d*, the difference between the bilayer thickness of the coating minus the bilayer thickness of the thickest coating, divided with the thickest coating, versus height on the sample mounting plate. The gray points are without any mask and the black points are with the mask. The measurements are made with 8 keV X-ray on 10 bilayer constant *d*-spacing coatings.

4. SUBSTRATE QUALITY

The flight substrate is 0.3 mm thick thermally slumped AF45 or D263 Schott glass[6] with radius between 40 mm and 120 mm and the length along the optical axes is 100 mm. Each mirror shell is divided into five mirror segments. The micro roughness of the flight substrate is critical for the quality of the flight coating. We have therefore made an extensive X-ray test of several hundred flight substrates. A small variation of the micro roughness of the glass on the order of ± 0.05 nm (RMS) has been observed. A typical example of a reflection curve of an uncoated flight mirror is shown in Fig. 2 and the fit gives a roughness of 0.36 nm.

5. UNIFORMITY

Because of inhomogenity in the magnets in the magnetrons and their finite length there will be thickness variations in the coating down along the sample mounting plates. To increase the area where the coating are homogeneous in thickness a mask have been designed, see Fig. 3a. Without the mask the thickness variation along a sample mounting plate was up to 60 %, see Fig. 3b. With the mask the thickness variation is less than 5 % for a 350 mm long area, without mask the variation in this area would be over 15 %. Outside the 350 mm area the variation with the mask were of the order of 40 %. It would be possible to get an even bigger homogeneous area but to do that the mask would need to make the opening even smaller with a decrease in coating rate as result. So the 350 mm homogeneous area is the best compromise between large coating area and high coating rate. Ideally the mask should be designed for each magnetron, each material, and for each separator plate distance (see next section) independently but the variation is small.

a

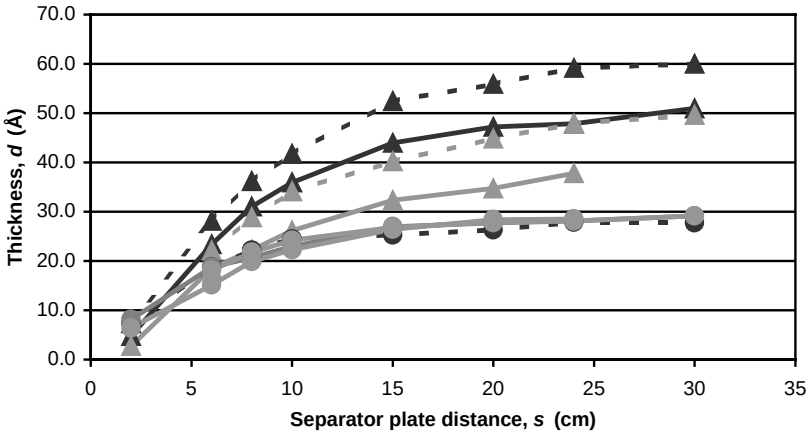

b

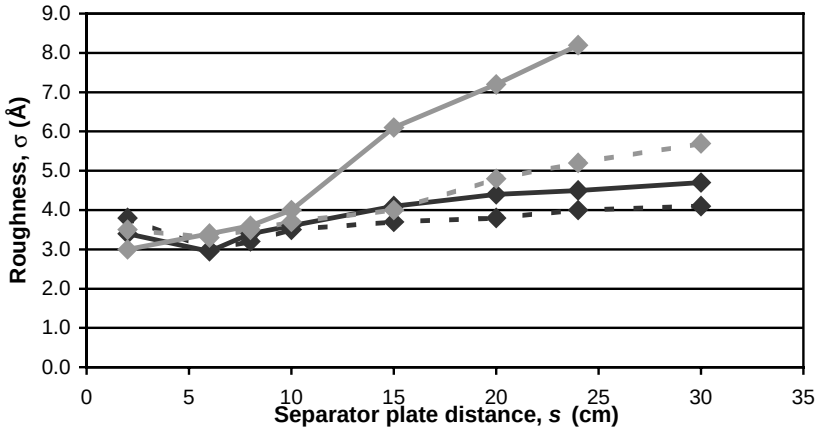

c

Fig. 4a: A side view of a sample mounting plate with four coated 100 mm long HEFT mirrors mounted. The mirrors are quintants with a radius of 51 mm. There are also mounted five 50 mm wide separator plates with 80 mm between them to collimate the material. b: Thickness of W and Si as function of separator plate distance and Ar pressure. The triangles are Si and the circles are W. c: Roughness of the coating as function of separator plate distance and Ar pressure. In both Fig. 4b and Fig. 4c the dotted black line is 0.33 Pa (2.5 mTorr), the solid black line is 0.47 Pa (3.5 mTorr), the dotted gray line is 0.53 Pa (4.0 mTorr), and the solid gray line is 0.80 Pa (6.0 mTorr). The measurements are made with 8 keV X-ray on 10 bilayer constant *d*-spacing coatings.

To check the homogeneity of the coating over a flight mirror we made constant *d*-spacing coatings and made reflection measurements on nine different points on the sample. The mirror was measured at the center position, at -20 degree, and at +30 degree azimuthally in the center of the optical axes and at the same angles ± 30 mm along the optical axes. We do see some small variation in the thickness over the sample. From 0 degree to ±20 degree we see no significant thickness variation but at ±30 degree the bilayer is up to 2% thinner. The same is true for ± 30 mm. This inhomogenity in thickness do not have any measurable effect on the graded *d*-spacing flight coating.

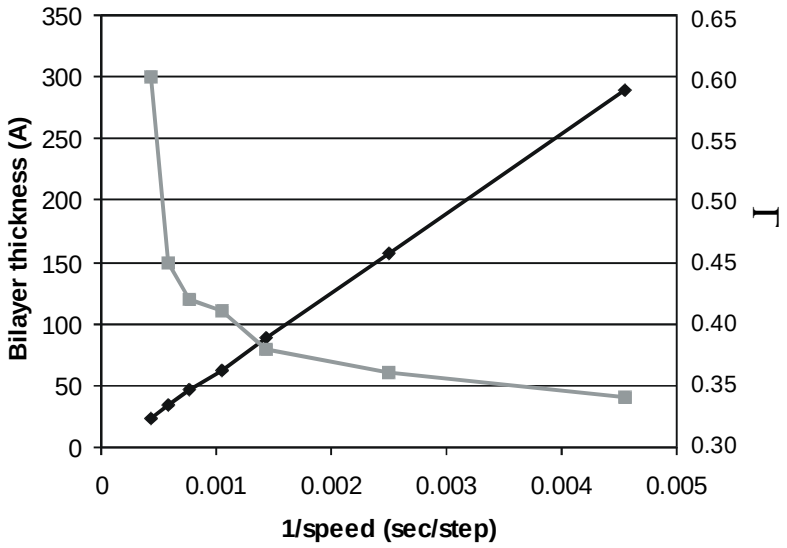

Fig. 5: The black line is the bilayer thickness versus one over speed and the gray line is Γ versus one over speed. The measurements are made with 8 keV X-ray on 10 bilayer constant *d*-spacing coatings.

6. INTERFACIAL ROUGHNESS

To decrease the roughness of the coating we are collimating the sputtered material with 50 mm wide separator plates that are mounted on the sample mounting plates, see Fig. 4a. By doing this, the sample only sees a part of the cathode and that decreases the coating rate but also the roughness. Fig. 4b shows a clear dependency of the thickness of both W and Si on the distance between separator plate, the closer together the separator plates are the lower is the coating rate. The figure also shows that the thickness of W do not depend of the Ar pressure between 0.33 Pa and 0.80 Pa but that the thickness of Si do, higher Ar pressure lower Si coating rate. Fig. 4c shows that the roughness increases with both increasing separator plate distance and with increasing Ar pressure.

Both Fig. 4b and Fig. 4c clearly shows that low Ar pressure is desireable. The lower the Ar pressure is the fewer collisions there will be between the Si atoms and the Ar atoms. That results in higher coating rate of Si, which is the limiting parameter in the coating time, and it decreases the roughness of the coating. Because W atoms are much heavier than Ar atoms a collision between the two do not effect the W atoms. As long that the Ar pressure is below 0.53 Pa and the separator plate distance is below 150 mm the effect of the Ar pressure on the roughness and therefore the quality of the coating is not big. The effect on the Si coating rate and therefore on the total coating time is more pronounced, Fig. 4b. The plasma in front of W ignites at 0.40 Pa (3.0 mTorr) and the plasma in front of Si ignites at 0.47 Pa (3.5 mTorr). After the plasma is ignited the Ar pressure can be lowered and the plasma will run stable but if the plasma dies because of arcing will not ignite again. Because a flight coating takes many hours it is important that the plasma will self ignite and therefore we operate at 0.49 Pa (3.7 mTorr) when making a flight coating.

Another way to decrease the possibility of collisions between Si atoms and Ar atoms it to decrease the target sample distance to a minimum dictated by the geometry of the chamber and such that the plasma do not shorten out on the samples. In our chamber the separator plates are 50 mm wide and the distance between target and the mask is 48 mm. Therefore the target to sample distance in our chamber is 108 mm. There need to be a little space between the mask and the separator plate because of the wide of the mask and because the sample mounting plates are mounted on a ring.

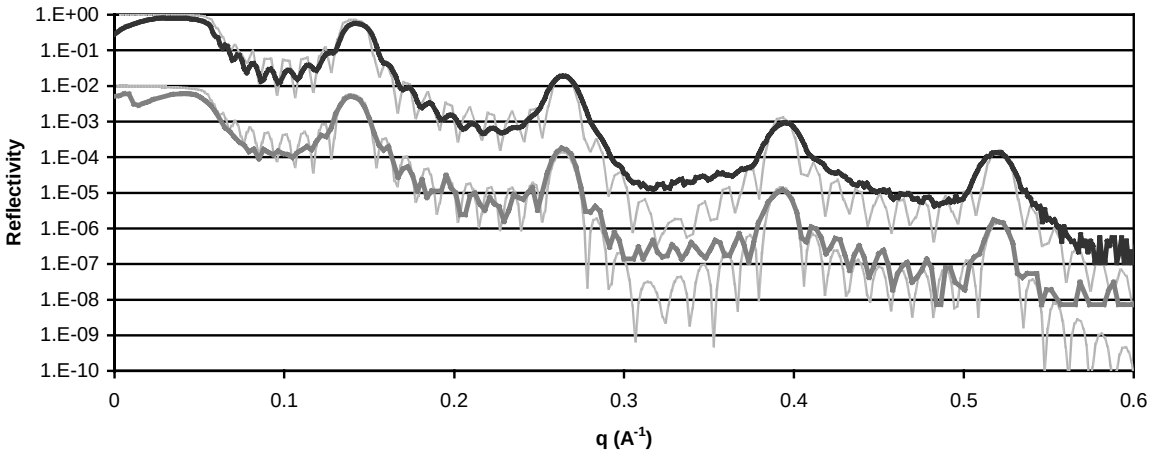

Fig. 6: The same 10 bilayer constant d-spacing coating measured with 40 keV (black line) and 8 keV (dark gray line). The 8 keV data are shifted two orders of magnitude for clarity. The plot shows reflectivity versus $q=4\pi \sin\Theta/\lambda$ where Θ is the incidence angle and λ is the X-ray wavelength. The light gray lines are fitted curves, the bilayer thickness is 4.85 nm and the roughness is 0.38 nm. First the fit were done to the 40 keV data and only the energy was changed for the light gray curve on the 8 keV data, all other variables were held constant.

The combination of the number of mounting plates, homogeneous coating area caused by the mask, and the distance between the separator plates define the total area that can be coated in one run. For shell 1 to 18 on the telescope (shell 1 is the innermost shell on the telescope) the separator plate distance is 80 mm and there can be 4 samples on each mounting plate resulting in 64 mirrors or a totally coated area of 0.44 m^2. For shell 19 to 32 the separator plate distance is 100 mm resulting in 3 samples per mounting plate, in all 48 samples or 0.42 m^2. From shell 33 to 55 the separator plate distance is 120 mm, there can still be 3 samples on a mounting plate so in total 48 mirrors in a coating run correspond to a coated area of 0.58 m^2. For shell 56 to 72 the separator plate distance is 145 mm leaving 2 samples on each mounting plate, in total 32 mirrors or a coated area of 0.48 m^2. The total coating thickness is smallest for the inner shells (~0.5 μm) and up to ~1.0 μm further out. Because the coating rate increases with increasing separator plate distance, Fig. 4b, the total coating time vary between 8 hours and 11 hours for all the mirror groups.

7. CALIBRATION DATA

A 10 bilayer constant *d*-spacing coating is very sensitive to thickness variation of the coating and is therefore used when making the calibration coatings. From the reflectivity data (an example is shown in Fig. 6) the bilayer thickness, Γ, and the roughness can be calculated. The result of a calibration coating is shown in Fig 5 where both the bilayer thickness and Γ are plotted. The bilayer thickness only depends on the rotation speed of the sample mounting plate so the thickness should be inverse proportional with the rotation speed, as seen in Fig. 5. There is also a dependency of Γ versus the inverse speed, the thicker a coating is the lower is the W fraction of the coating. The coating design is made with a constant Γ but the Γ variation that is seen in Fig. 5 actually increase the overall throughput with about 2 %[9].

We did some single layer Si coatings on glass, measured the thickness, and compared this to the thickness of Si from 10 bilayer W/Si coatings done with the same rotation speeds. At every speed we saw that the W resputtered 4.7 nm Si with the coating parameters we are using. There is no resputtering of W.

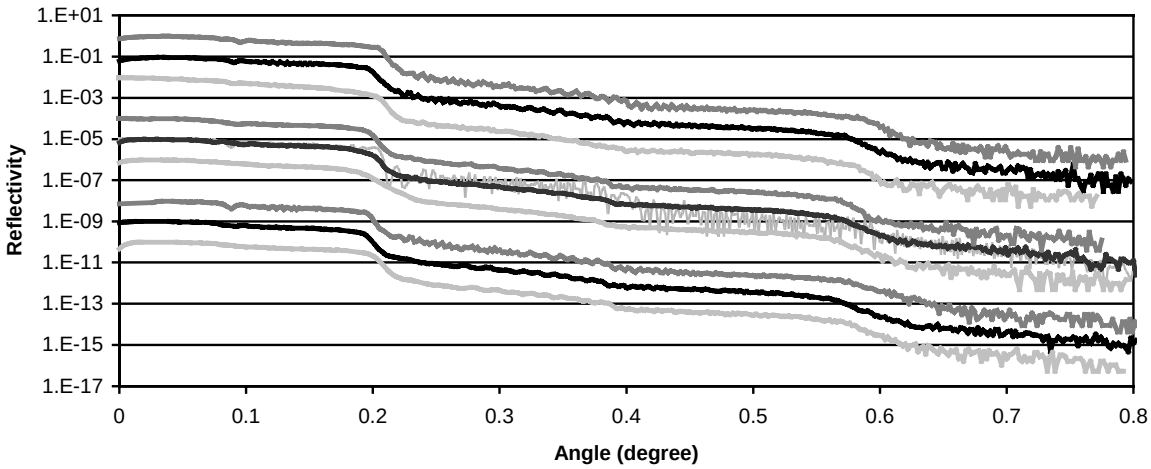

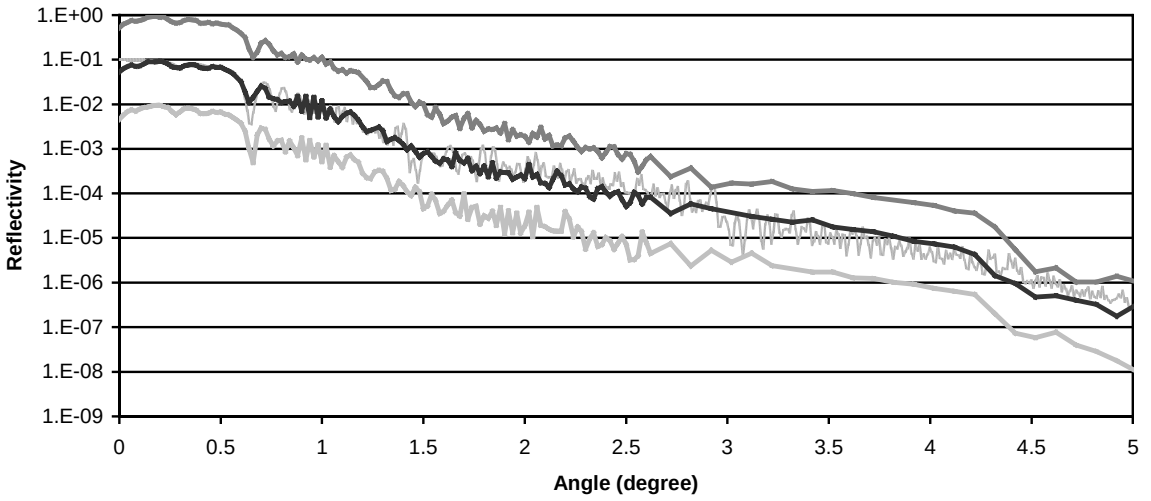

Fig. 7a: The reflectivity as function of gracing incidence angle measured with 60 keV on nine different positions. The curves are shifted in the y-direction for clarity. The coating is a graded *d*-spacing flight coating for the inner HEFT shells. The center of the sample is defined as 0 mm length and 0 degrees in azimuth angle. The black lines are measured at 0 degree azimuthal, the dark gray at +30 degree, and the light gray at -20 degree at there different length on the optical axes. The top three lines are measured at 30 mm from the center, the center three lines are measured at the center and the three last lines are measured at -30 mm. The gray line on the 0 degree 0 length curve is a fit to the data with the nominal power law distribution d_{min} = 2.97 nm, d_{max} = 29.76 nm, Γ = 0.393, c = 0.236, and roughness of 0.34 nm. b: The same sample as above measured at 8 keV. Here are curves at 0 mm length for 30 degree (dark gray), 0 degree (black), -20 degree (light gray), and the fitted curve.

8. HIGH ENERGY REFLECTANCE MEASUREMENTS

The coating of flight mirrors for HEFT has started and we are through about 25 % of the shells for the first HEFT module. All our calibration samples are measured at 8 keV and a test sample from every flight coating is tested to see

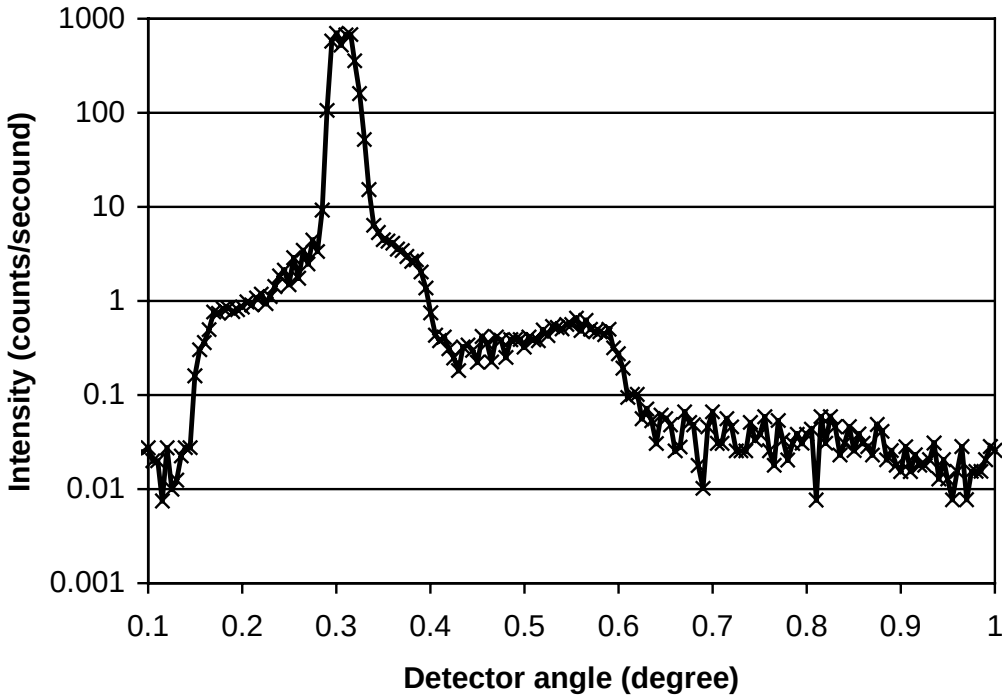

Fig. 8: Scatter measurements of a flight mirror coated for the inner HEFT shells measured at 60 keV. The incidence angle was 0.15 degree.

that the coating have the required quality. To ensure that we have a good understanding of how the mirror quality is at the X-ray energies for which the coating are designed we have tested some of our flight coatings at the European Synchrotron Radiation Facility (ESRF) at higher energies at beamline BM05.

To show that our day to day X-ray measurements corresponds to higher energy measurements Fig. 6 shows the same coating measured with 8 keV and 40 keV X-ray. The light gray line is the fit to the 40 keV data and gives a bilayer thickness of 4.85 nm and a roughness of 0.38 nm. Then the only parameter changed was the X-ray energy and we see a perfect fit to the 8 keV data. The data was taken on the same spot on the sample.

We have measured a coated flight mirror on nine locations, see Fig. 7a. The mirror was measured at the center position, at -20 degree, and at +30 degree azimuthally in the center of the optical axes and at the same angles ± 30 mm along the optical axes. There is very little variation between the nine curves indicating that the coating is homogeneous over the sample. The fit to the measured points in the middle of the sample shows that this coating has a roughness of 0.34 nm. Fig. 7b shows the same mirror measured at +30 degree, 0 degree, and -20 degree azimuthally in the center of the optical axes with 8 keV X-ray. Again there are only small variations between the curves and the fit is in good agreement with the experimental data.

9. SCATTER DATA

To measure the scatter from a HEFT flight mirror, the sample is aligned at a given fixed incidence angle while the detector scans through the scattered beam. The resolution achieved with the setup at the BM05 is 0.001 degree (4

arcsecond). Fig. 8 shows a measurement done at 60 keV and fixed grazing incidence angle of 0.15 degree. The specular reflection is expected at 0.30 degree, two times the incidence angle. The background level is 0.05 counts per seconds. The width of the specular peak is due to figure error resulting mainly from imperfect mounting. The intensity levels seen on each side of the peak are from true scatter. Less than 2% of the intensity is scattered outside the specular peak which demonstrates that the true scatter contributes insignificantly to the imaging properties.

10. CONCLUSION

The production of flight optic for the HEFT balloon experiment has started and about 25 % of the glass segments for the first telescope has been coated. The coating facility and coating design have been described and we have shown that both the quality and homogeneity for the flight coatings are meeting the requirements for HEFT and future hard X-ray missions.

11. REFERENCES

1. F. A. Harrison et al, "Development of the High-Energy Focusing Telescope (HEFT) balloon experiment," SPIE Vol. 4012, pp. 693-699, 2000.
2. F. E. Christensen et al, "A graded d-spacing multilayer telescope for high energy X-ray Astronomy," SPIE Vol. 1546, pp. 160-167, 1991.
3. D. L. Windt et al, "Growth, structure and performance of depth-grated W/Si multilayers for hard X-ray optics," J. Applied Physics, Vol. 88, pp. 460-470, 2000.
4. C. J. Hailey et al, "Investigation of substrates and mounting techniques for the High Energy Focusing Telescope (HEFT)," SPIE Vol. 3114, pp. 535-543, 1997.
5. W. W. Craig et al, "Hard X-ray Optics for the HEFT Balloon Borne Payload: Prototype Design & Status," SPIE Vol. 3445, pp. 112-120, 1998.
6. J. Koglin et al, "Development and production of hard X-ray multilayer optics for HEFT," SPIE Vol. 4851 (2002).
7. C. P. Jensen et al, "Multilayer coating facility for the HEFT hard X-ray telescope," SPIE Vol. 4496, pp104-108, 2002.
8. K. D. Joensen et al, "Design of grazing-incidence multilayer supermirrors for hard X-ray reflectors," Applied Optics, Vol. 34, pp. 7935-7944, 1995.
9. P. H. Mao et al, "Optimization of graded multilayer designs for astronomical x-ray telescopes," Applied Optics, Vol. 38, pp. 4766-4775, 1999.